Electrocatalysis (2016) 7:121–126
DOI 10.1007/s12678-015-0290-x

ORIGINAL RESEARCH

Cathodic Evolution of Hydrogen on Platinum-Modified Nickel Foam Catalyst

Boguslaw Pierozynski[1] · **Tomasz Mikolajczyk**[1]

Published online: 4 November 2015

Abstract This paper reports on cathodic evolution of hydrogen, examined at Pt-modified nickel foam material. Hydrogen evolution reaction (HER) was studied in 0.1 M NaOH solution on platinum-activated nickel foam catalyst material, obtained via a spontaneous deposition method. Catalytic Pt modification of nickel foam resulted in a substantial enhancement of the HER kinetics, as compared to those recently recorded on Pd/Ru-modified Ni foam catalyst materials. Electrochemical investigations were carried out by means of AC impedance spectroscopy and quasi-potentiostatic cathodic polarization experiments. In addition, importance of nano-catalytic nature of the Pt deposit and its influence on the HER characteristics were discussed in detail with help of SEM/EDX spectroscopy analysis.

Keywords Nickel foam · Pt modification · HER · Impedance spectroscopy

Introduction

Cathodic evolution of hydrogen on metal-based catalysts provides hydrogen gas of superior purity, which is extremely important for proton exchange membrane (PEM) fuel cells applications. Nickel itself is well known as a highly reactive (and corrosion-resistant) material for hydrogen evolution reaction (HER) in alkaline media [1–3]. However, especially important are structures having large specific surface area, such as nickel foam-based catalyst materials [4, 5]. Nickel foams are extremely valuable as they provide high porosity and large specific surface area electrocatalyst with superior electrical conductivity and mechanical characteristics [5, 6].

Significant improvement of electrocatalytic HER properties of nickel foam could conveniently be realized through surface deposition of nano-structured noble metals. This might be performed via electrodeposition, spontaneous deposition [5, 7, 8], or by chemical reduction processes, where the latter is typically carried out with $NaBH_4$, ethylene glycol, hydrazine, or their mixtures [9–13]. In this work, the HER characteristics of Pt-modified nickel foam (via spontaneous deposition) are presented, also comparatively to those of palladium/ruthenium-activated Ni foam samples, as recently illustrated in another publication from this laboratory [14].

Research Highlights • Pt deposition radically enhanced HER kinetics of Ni foam.
• Pt modifies electrochemically active surface of nickel foam.
• Pt-modified Ni foam cathodes for alkaline water electrolysers.

✉ Boguslaw Pierozynski
bogpierozynski@yahoo.ca; boguslaw.pierozynski@uwm.edu.pl

[1] Department of Chemistry, Faculty of Environmental Management and Agriculture, University of Warmia and Mazury in Olsztyn, Plac Lodzki 4, 10-957 Olsztyn, Poland

Experimental

Solutions, Chemicals, Electrochemical Cell, and Electrodes

All electrolytes were made up from ultra-pure water, produced by means of Direct-Q3 UV water purification system from Millipore (18.2 MΩ cm water resistivity). 0.1 M NaOH supporting solution was prepared from AESAR, 99.996 % NaOH pellets, whereas 0.5 M H_2SO_4 (SEASTAR Chemicals, BC, Canada) solution was used for intermittent charging of a Pd reversible hydrogen electrode. An electrochemical cell, made of Pyrex glass, was used during the course of this work. It comprised three electrodes: a Ni foam-based working

electrode (WE) in a central part, the reversible Pd hydrogen electrode (RHE) as reference and a Pt counter electrode (CE), both placed in separate compartments. Before performing the HER experiments, each Ni foam electrode was activated in 0.1 M NaOH by cathodic polarization at 20 mA for 300 s in order to remove any spontaneously formed Ni oxide layer.

Nickel foam was purchased from MTI Corporation (purity, >99.99 % Ni; thickness 1.6 mm; surface density, 346 g m^{-2}; porosity, ≥95 %). Spontaneous deposition of Pt (see details on the spontaneous Pd/Ru deposition on Ni foam substrate given in [14]) on nickel foam samples (*ca.* 1.1×1.1 cm) was carried out from chloroplatinic acid hexahydrate (CPAH, Sigma-Aldrich) solution [electrode **A**: 0.005 M CPAH, pH=3.0, $t_{dep.}$= *120 s (deposition time),* $T_{dep.}$=293 K (deposition temperature), m_s=41.3 mg (sample mass) with estimated 0.23± 0.02 wt.% Pt; electrode **B**: 0.0005 M CPAH, pH=1.0, $t_{dep.}$= 30 s, $T_{dep.}$=293 K, m_s=41.2 mg with estimated 0.18± 0.02 wt.% Pt]. All information concerning specific pretreatments applied to samples of Ni foam, details on the reference and counter electrodes, as well as those on electrochemical cell preparation were also given in [14].

Experimental Methodology

AC impedance spectroscopy and quasi steady-state polarization techniques were employed in this work. All electrochemical measurements were carried out at room temperature (293 K) by means of the *Solartron* 12,608 W Full Electrochemical System, consisting of 1260 frequency response analyzer (FRA) and 1287 electrochemical interface (EI). For the AC impedance measurements, the generator provided an output signal of 5 mV rms and the frequency range was swept between 1.0×10^{5} and 0.5×10^{-1} Hz. The instruments were controlled by *ZPlot 2.9* or *Corrware 2.9* software for Windows (Scribner Associates, Inc.). Typically, three impedance measurements were performed at each potential value, independently at two foam electrodes, where reproducibility of such obtained results was usually below 10 %. Data analysis was performed with *ZView 2.9* (*Corrview 2.9*) software package, where the impedance spectra were fitted by means of a complex, nonlinear, least squares immittance fitting program, *LEVM 6*, written by J.R. Macdonald [15]. In addition, quasi-potentiostatic cathodic polarization experiments for the HER were performed at selected Pt-modified Ni foam electrodes. They were recorded at a scan rate of 0.5 mV s^{-1}. On the other hand, SEM/EDX spectroscopic characterization of all studied Pt-based Ni foam electrodes was conducted by means of JEOL JSM-7600 F/X-Max SDD Oxford Inca 250 integrated SEM/EDX equipment unit.

Results and Discussion

SEM/EDX Characterization of Pt-Activated Nickel Foam Electrodes

Figure 1a presents SEM micrograph pictures of electrode **A**, recorded in a sequence of magnifications (×250, ×2000, ×10,000, and ×50,000, at an acceleration voltage of 2 kV), where the presence of homogeneously distributed small Pt nuclei could clearly be observed. On the other hand, Fig. 1b, c demonstrates Pt detection on the Ni foam substrates, achieved by the SEM/EDX analysis for the electrode **A** (0.23 wt.% Pt) and electrode **B** (0.18 wt.% Pt) catalyst samples, correspondingly.

Quantities of the deposited Pt catalyst on the nickel foam substrate were assessed by means of a weighing method, where amounts of nickel dissolved during the Pt deposition process were spectroscopically estimated (via a complexometric method [16] by means of WTW Photo Flex Turb spectrometer). In addition, SEM-estimated (see [17 and 18] for details) Pt average grain size came to 12.4±4.2 nm and 9.1±3.1 nm for the electrodes **A** and **B**, respectively.

AC Impedance Performance of HER on Pt-Modified Ni Foam Materials in 0.1 M NaOH

AC impedance characterization of the HER on both examined Pt-modified Ni foam electrode types in 0.1 M NaOH is shown in Fig. 2 and Table 1. Thus, the impedance-examined, Pt-activated Ni foam electrodes exhibited single, "depressed" semicircles (a single-step charge-transfer reaction) at all studied potential values, in the explored frequency range (see examples of Nyquist impedance plots recorded at −100 mV in Fig. 2). The overpotential dependence of Faradaic reaction resistance (R_{ct}) and double-layer capacitance (C_{dl}) parameters for the HER (derived based on a constant phase element—CPE-modified Randles equivalent circuit model shown in Fig. 3) are presented in Table 1. The CPE element was included in the circuit in order to account for the capacitance dispersion [19, 20] effect, represented by distorted semicircles in the Nyquist impedance plots (see Fig. 2 again). It should be stressed here that a high-frequency semicircle (a typical electrode porosity response) was practically indiscernible in most of the Nyquist impedance plots. In fact, application of a two-time constant equivalent circuit (see Fig. 4b in [14]) would lead here to significant errors on such derived electrochemical parameters.

Thus, for the Pt-activated Ni foam electrode produced at pH 3.0 (electrode **A**), the recorded R_{ct} parameter reduced from 1.046 Ω g at −50 mV to 0.205 Ω g at −350 mV vs. RHE. At the same time, the derived C_{dl} parameter came to 19,846 and 16,122 μF g^{-1} $s^{\varphi 1-1}$ for the corresponding potential values. In fact, these values of the charge-transfer resistance are fairly close to those recently recorded for the HER on Pd and Ru-

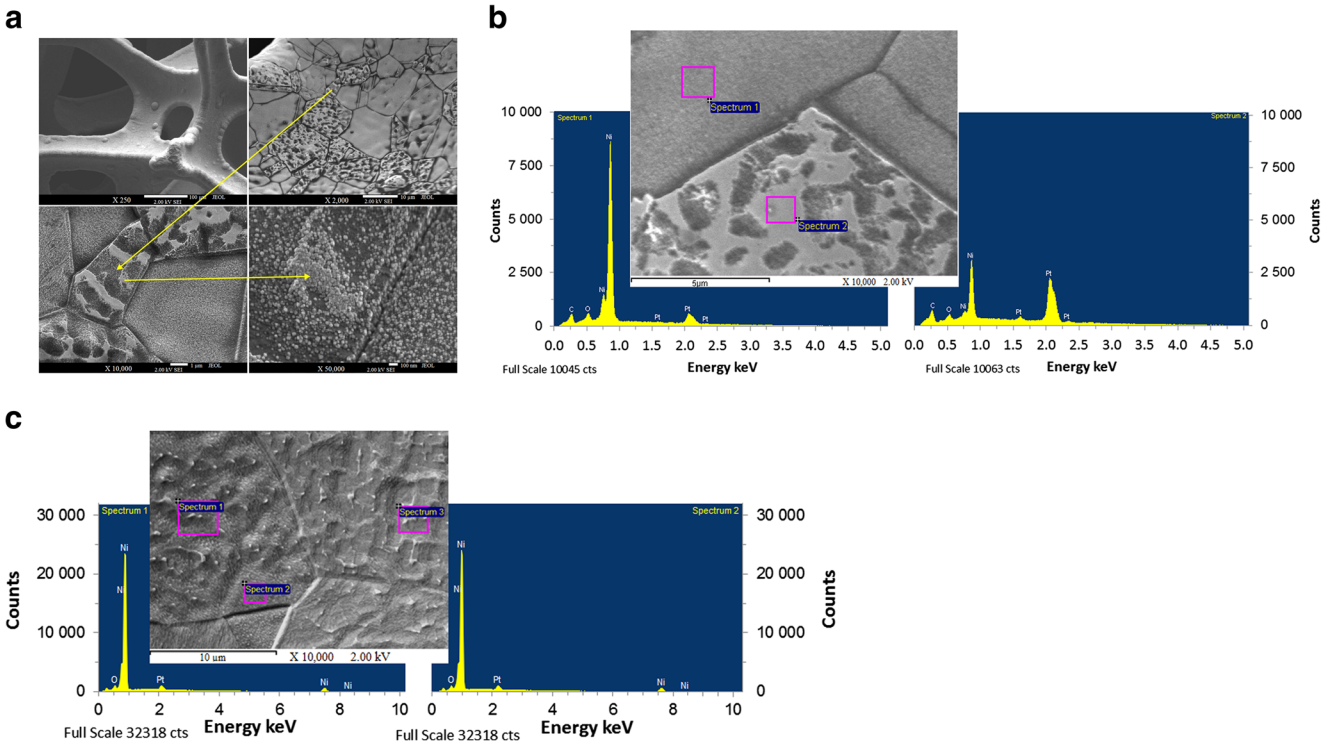

Fig. 1 **a** SEM micrograph pictures of Pt-modified Ni foam surface (electrode **A**), taken at ×250, ×2000, ×10,000, and ×50,000 magnifications; **b** SEM picture (taken at ×10,000 magnification)/EDX spectrum for Pt-modified Ni foam surface (electrode **A**); **c** As in **b**, but for electrode **B**

modified nickel foam electrodes under analogous experimental conditions (see Ref. [14] for details). In contrast, the C_{dl} parameter values recorded here at −50 mV accounted for *ca.* 11 and 21 % of those recorded for the Pd and Ru-modified Ni foam electrodes, implying that platinum offers significantly enhanced catalytic HER properties, as compared to those exhibited by Pd and Ru elements. The above is apparently in good agreement with former findings on the subject with respect to the fact that Pt possesses superior catalytic properties to other HER highly active elements of the periodic table [21–23].

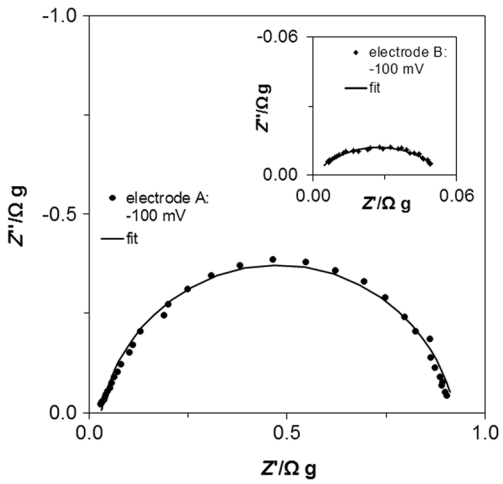

Fig. 2 Complex-plane impedance plots for the HER on Pt-modified Ni foam electrode surfaces in contact with 0.1 M NaOH, recorded at room temperature for the potential of −100 mV (vs. RHE). The solid lines correspond to representation of the data according to equivalent circuit shown in Fig. 3

Interestingly, substantially enhanced HER catalysis was recorded on the electrode **B**, obtained by spontaneous Pt deposition (0.18 wt.% Pt) on the Ni foam substrate, but at significantly reduced pH value of 1.0. Here, the R_{ct} parameter reached 0.067 Ω g at −50 mV and 0.040 Ω g at −350 mV vs. RHE, while the recorded values of the interfacial capacitance parameter came to 1,214,805 and 126,259 µF g^{-1} $s^{\varphi 1-1}$ for the corresponding potential values (a dramatic drop of the C_{dl} reflects partial blocking of electrochemically accessible surface area of the electrode by freshly formed hydrogen microbubbles at extended cathodic overpotentials [14]). Hence, it could be assumed that at significantly more acidic conditions, the process of in situ activation of Ni foam (including surface oxide removal) is much more efficient than that for the electrode **A**, under the pH value of 3.0. As a consequence, the catalyst deposition is considerably faster (see Experimental, paragraph 2.1.) and such produced Pt surface deposits (electrode **B**) tend to be substantially more homogeneous and considerably smaller in grain size (see Fig. 1a, c). In addition, dimensionless φ parameter (φ determines the constant phase angle in the complex-plane plot, where $0 \leq \varphi \leq 1$) of the CPE circuit (Fig. 3) varied between 0.84–0.88 and 0.45–0.81 (see inset to Fig. 2) for the electrodes **A** and **B** correspondingly. Significant increase of the φ parameter (from 0.45 to 0.81) upon overpotential augmentation for

Table 1 Electrochemical parameters for the HER, obtained on Pt-modified Ni foam electrodes in contact with 0.1 M NaOH

E/mV	R_{ct}/Ω g	C_{dl}/μF g^{-1} $s^{\varphi-1}$
Electrode A		
−50	1.046±0.004	19,846±136
−100	0.894±0.006	19,969±1634
−150	0.655±0.015	18,389±1422
−200	0.473±0.006	16,446±894
−250	0.347±0.005	15,944±1226
−300	0.261±0.001	14,727±1685
−350	0.205±0.003	16,122±1307
Electrode **B**		
−50	0.067±0.002	1,214,805±112,509
−100	0.056±0.001	682,063±39,793
−150	0.053±0.001	547,791±61,798
−200	0.048±0.001	262,597±38,864
−250	0.046±0.001	268,713±32,245
−300	0.040±0.001	158,082±17,068
−350	0.040±0.004	126,259±30,302

The results were obtained by fitting the CPE-modified Randles (Fig. 3) equivalent circuit to the experimentally obtained impedance data (reproducibility typically below 10 %, $\chi^2 = 5\times10^{-5}$ to 2×10^{-3}); φ (electrode **B**) 0.45, 0.52, 0.56, 0.67, 0.81, 0.80 and 0.81 for η rising from −50 to −350 mV vs. RHE, respectively

the electrode **B** is predominantly a result of more extensive accumulation of H_2 microbubbles within irregular entity of the electrode surface.

It should be mentioned that the impedance results presented here for the Pt-modified nickel foam electrodes were significantly enhanced, as compared to those reported on unmodified Ni foam materials in [14] and [24] (with the recorded R_{ct} parameter values of about 1.10–1.30 Ω g at −200 mV and 0.55 Ω g at −250 mV).

Moreover, the exchange current density values (j_0) for the HER on the Pt-modified nickel foam samples were calculated based on the linear relationship: −log R_{ct} vs. η/overpotential

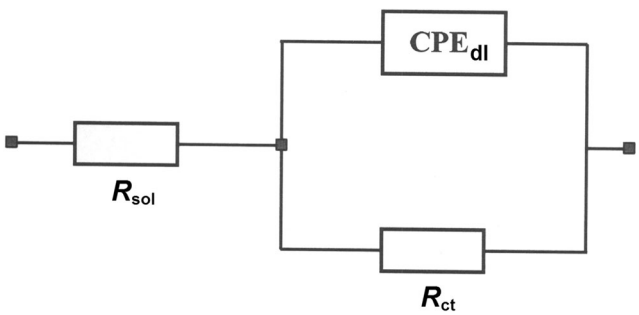

Fig. 3 Equivalent circuit model used for fitting the impedance data for Pt-modified Ni foam electrodes, obtained in 0.1 M NaOH. The circuit includes a constant phase element (*CPE*) for distributed capacitance; R_{ct} and C_{dl} (as CPE_{dl}) elements correspond to the HER charge-transfer resistance and double-layer capacitance components, and R_{sol} is solution resistance

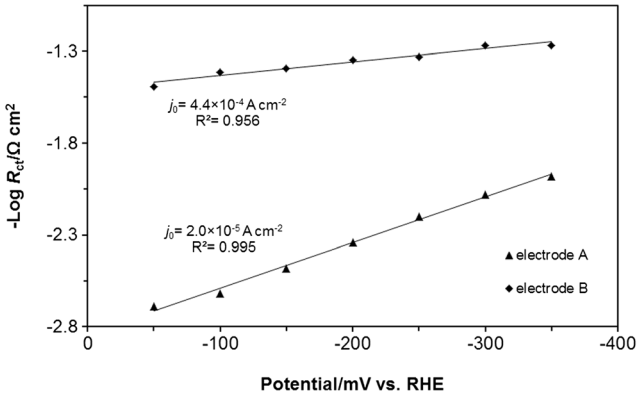

Fig. 4 - Log R_{ct} vs. overpotential relationship for the HER, studied in 0.1 M NaOH on Pt-activated Ni foam electrodes (*symbols* represent experimental results)

(here, η ranged from −50 to −350 mV RHE), satisfied for kinetically controlled reactions by utilizing the Butler-Volmer equation and the relation between the j_0 and the R_{ct} parameter for η approaching 0 [25–27]. Thus, the calculated j_0 values came to 2.0×10^{-5} and 4.4×10^{-4} A cm^{-2} for the electrodes **A** and **B** (Fig. 4), respectively. Although the former catalyst exhibited similar j_0 value to that recently [14] recorded on the Pd-modified nickel foam (2.2×10^{-5} A cm^{-2}), the exchange current density recorded for the latter one was greatly increased, as compared to those derived on both the Pd and Ru-activated Ni foam electrodes. It should also be noted that electrochemically active surface area of the Ni foam samples was estimated here at *ca*. 17.1 cm^2, based on the procedure given in Ref. [14].

Tafel Polarization Curves

The impedance results discussed above are in good agreement with these of the potentiostatic Tafel polarization plots, shown in Fig. 5. Here, the recorded cathodic slopes (b_c) approached

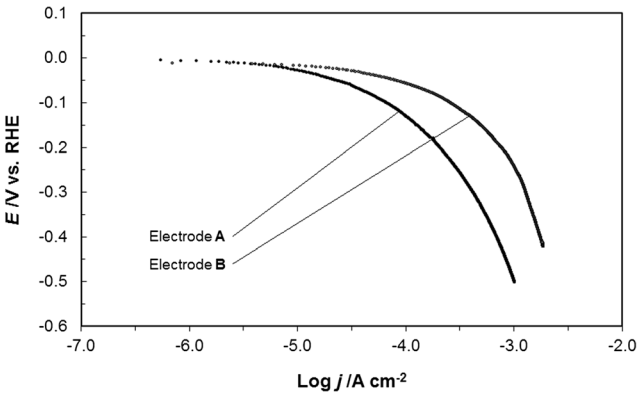

Fig. 5 Quasi-potentiostatic cathodic polarization curves (recorded at a rate of 0.5 mV s^{-1}) for the HER on Pt-modified Ni foam electrode surfaces (electrodes **A** and **B**), carried out in 0.1 M NaOH solution (appropriate *iR* correction was made based on the solution resistance derived from the impedance measurements); calculated Tafel slopes, b_c=70 and 73 mV dec^{-1} for electrode **A** and electrode **B**, respectively

70 and 73 mV dec^{-1} for the electrodes **A** and **B**, respectively (compare with similar values obtained on the Pd and Ru-modified Ni foam samples in Ref. [14]). Furthermore, the corresponding Tafel-based j_0 parameter values for the HER came to 1.3×10^{-5} (electrode **A**) and 5.4×10^{-5} A cm^{-2} (electrode **B**). Significant difference between the Tafel-calculated and the impedance-derived values of the j_0 parameter results from the fact that a linear Tafel region for the studied Ni foam-based catalysts was not very well pronounced. Hence, the Tafel-based data presented here should only be considered qualitatively.

Nevertheless, superior catalytic nature of the electrode **B** could clearly be revealed in Fig. 5 when one makes a comparison of the recorded current densities at fixed overpotential values. Hence, for the overpotential of −100 mV, the current densities came to 6.8×10^{-5} and 2.6×10^{-4} A cm^{-2} for the electrode **A** and electrode **B**, respectively. Then, at the overpotential of −300 mV, the resulting current densities approached 4.2×10^{-4} and 1.3×10^{-3} A cm^{-2}, correspondingly.

Interestingly, analogous HER studies performed on Pt-activated (fully characterized [28]), CVD-produced nickel foam [29, 30] and a 3-D porous Ni electrode structure [31] resulted in Tafel slopes on the order of 90 to 159 mV dec^{-1} and exchange current densities of 3.9×10^{-4} [30] and 9.5×10^{-3} A cm^{-2} [31].

Finally, electrocatalytic HER performance of the Pt-modified Ni foam electrodes ("normalized" via the surface area estimates given through interfacial capacitance measurements) compares quite well with those of other HER works [8, 32–35], carried out on similar, large surface area and highly porous (spongy type) catalyst materials. However, it might be difficult to make direct comparisons of catalytic properties of those materials with the Pt-activated nickel foam cathodes described in this work. In fact, in some of these papers [8, 32, 34, 35], electrochemical parameters for modified catalyst materials are reported with respect to initial surface area of unmodified electrodes, thus yielding a tremendous (several orders in magnitude), but surface unadjusted enhancement of the HER activity.

Conclusions

Platinum is well known to exhibit superior catalytic properties towards cathodic evolution of hydrogen. Pt nanoparticle-modified (at *ca*. 0.2 wt.% Pt) nickel foam provides a highly active catalyst material for HER in 0.1 M NaOH medium, which understandably outperforms those of Pd and Ru-modified Ni foam materials obtained by a similar, spontaneous metal deposition route.

Nevertheless, electrocatalytic HER properties of Pt-activated nickel foam are largely modifiable during the catalyst deposition process. Here, especially valuable proved to be the kinetic results recorded on the Pt-modified Ni foam substrate, produced under enhanced acidic conditions (electrode **B**). Thus, in situ facilitation of substrate activation process resulted in considerably more homogeneous distribution of the Pt nanodeposits. Such obtained catalyst exhibited considerably improved HER properties, based on extended electrochemically active surface area, as compared to that prepared under "regular" pH conditions (electrode **A**).

Finally, preliminary results obtained in this work unambiguously indicated substantial opportunities for the application of Pt-modified nickel foam cathodes in alkaline water electrolysis.

References

1. B.E. Conway, B.V. Tilak, Adv Catalysis **38**, 1 (1992)
2. J.Y. Huot, L. Brossard, Int J Hydrogen Energy **12**(12), 821 (1987)
3. H.E.G. Rommal, P.J. Morgan, J Electrochem Soc **135**(2), 343 (1988)
4. H. He, H. Liu, F. Liu, K. Zhou, Surf Coat Technol **201**, 958 (2006)
5. E. Verlato, S. Cattarin, N. Comisso, A. Gambirasi, M. Musiani, L. Vazquez-Gomez, Electrocatalysis **3**, 48 (2012)
6. S. Inazawa, A. Hosoe, M. Majima, K. Nitta, SEI Tech Rev **71**, 23 (2010)
7. I. Bianchi, E. Guerrini, S. Trasatti, Chem Phys **319**, 192 (2005)
8. L. Vazquez-Gomez, S. Cattarin, P. Guerriero, M. Musiani, Electrochim Acta **53**, 8310 (2008)
9. P. Kim, J.B. Joo, W. Kim, J. Kim, I.K. Song, J. Yi, J Power Sources **160**, 987 (2006)
10. Y. Suo, I.M. Hsing, J Power Sources **196**, 7945 (2011)
11. A. Dutta, S.S. Mahapatra, J. Datta, Int J Hydrogen Energy **36**, 14898 (2011)
12. R.M. Modibedi, T. Masombuka, M.K. Mathe, Int J Hydrogen Energy **36**, 4664 (2011)
13. B. Beyribey, B. Corbacioglu, Z. Altin, GUJS **22**(4), 351 (2009)
14. B. Pierozynski, T. Mikolajczyk, I.M. Kowalski, J Power Sources **271**, 231 (2014)
15. J.R. Macdonald, *Impedance Spectroscopy, Emphasizing Solid Materials and Systems* (John Wiley & Sons, New York, 1987)
16. C. Santos de Souza, M. Korn, Anal Chim Acta **444**, 309 (2001)
17. B. Pierozynski, T. Mikolajczyk, Electrocatalysis **6**, 51 (2015)
18. B. Pierozynski, T. Mikolajczyk, M. Turemko, E. Czerwosz, M. Kozlowski, Int J Hydrogen Energy **40**, 1795 (2015)
19. T. Pajkossy, J Electroanal Chem **364**, 111 (1994)
20. B.E. Conway, B. Pierozynski, J Electroanal Chem **622**, 10 (2008)
21. B.E. Conway, B.V. Tilak, Electrochim Acta **47**, 3571 (2002)
22. J. Barber, S. Morin, B.E. Conway, J Electroanal Chem **446**, 125 (1998)
23. J. Barber, B.E. Conway, J Electroanal Chem **461**, 80 (1999)
24. M. Grdeń, M. Alsabet, G. Jerkiewicz, ACS Appl Mater Interfaces **4**, 3012 (2012)

25. J.G. Highfield, E. Claude, K. Oguro, Electrochim Acta **44**, 2805 (1999)
26. R.K. Shervedani, A.R. Madram, Electrochim Acta **53**, 426 (2007)
27. S. Martinez, M. Metikos-Hukovic, L. Valek, J Mol Cat A: Chem **245**, 114 (2006)
28. J. van Drunen, B. Kinkead, M.C.P. Wang, E. Sourty, B.D. Gates, G. Jerkiewicz, ACS Appl Mater Interfaces **5**, 6712 (2013)
29. S. Fiameni, I. Herraiz-Cardona, M. Musiani, V. Perez-Herranz, L. Vazquez-Gomez, E. Verlato, Int J Hydrogen Energy **37**, 10507 (2012)
30. J. van Drunen, B.K. Pilapil, Y. Makonnen, D. Beauchemin, B.D. Gates, G. Jerkiewicz, ACS Appl Mater Interfaces **6**, 12046 (2014)
31. X. Qian, T. Hang, S. Shanmugam, M. Li, ACS Appl Mater Interfaces **7**, 15716 (2015)
32. C. Hitz, A. Lasia, J Electroanal Chem **500**, 213 (2001)
33. I. Herraiz-Cardona, E. Ortega, L. Vazquez-Gomez, V. Perez-Herranz, Int J Hydrogen Energy **37**, 2147 (2012)
34. L. Vazquez-Gomez, S. Cattarin, P. Guerriero, M. Musiani, Electrochim Acta **52**, 8055 (2007)
35. A.L. Antozzi, C. Bargioni, L. Iacopetti, M. Musiani, L. Vazquez-Gomez, Electrochim Acta **53**, 7410 (2008)